Inorganica Chimica Acta 395 (2013) 135–144

Contents lists available at SciVerse ScienceDirect

Inorganica Chimica Acta

journal homepage: www.elsevier.com/locate/ica

Synthesis and biological evaluation of *N*-heterocyclic carbene–silver(I) acetate complexes derived from 4,5-ditolyl-imidazole

Frauke Hackenberg, Grainne Lally, Helge Müller-Bunz, Francesca Paradisi, Daniela Quaglia, Wojciech Streciwilk, Matthias Tacke *

Centre for Synthesis and Chemical Biology (CSCB), UCD School of Chemistry and Chemical Biology, University College Dublin, Belfield, Dublin 4, Ireland

ARTICLE INFO

Article history:
Received 29 August 2012
Received in revised form 26 October 2012
Accepted 31 October 2012
Available online 14 November 2012

Keywords:
NHC–silver complexes
Caki-1
MCF-7
Escherichia coli
Staphylococcus aureus

ABSTRACT

From the reaction of 1,2-bis-(4-methylphenyl)ethane-1,2-dione with formamide, symmetrically substituted 4,5-bis-(4-methylphenyl)-1H-imidazole (**1**) was synthesised and further reacted with *p*-benzyl substituted halides to give the symmetrically substituted *N*-heterocyclic carbene (NHC) precursors **1a–e**.

The NHC precursors were then reacted with silver(I) acetate to yield NHC–silver(I) acetate complexes 1,3-bis-(benzyl)-4,5-bis-(4-methylphenyl)-imidazole-2-ylidene silver(I) acetate (**2a**), 1,3-bis-(4-methylbenzyl)-4,5-bis-(4-methylphenyl)-imidazole-2-ylidene silver(I) acetate (**2b**), 1,3-bis-(4-methoxylbenzyl)-4,5-bis-(4-methylphenyl)-imidazole-2-ylidene silver(I) acetate (**2c**), 1,3-bis-(4-methoxycarbonylbenzyl)-4,5-bis-(4-methylphenyl)-imidazole-2-ylidene silver(I) acetate (**2d**) and 1,3-bis-(4-cyanobenzyl)-4,5-bis-(4-methylphenyl)-imidazole-2-ylidene silver(I) acetate (**2e**).

Two NHC–silver acetate complexes **2a** and **2e** were characterised by single crystal X-ray diffraction. The preliminary *in vitro* antibacterial activity of the NHC–silver complexes **2a–e** was investigated against Gram-positive bacteria *Staphylococcus aureus* and Gram-negative bacteria *Escherichia coli* using the qualitative Kirby–Bauer disk-diffusion method. The areas of clearance determined for the maximum dose (4.3 μM) range between 1 mm and 7 mm for MSSA and 0 mm and 7 mm for *E. coli*. All of the newly synthesised silver(I) acetate complexes were tested for their cytotoxicity by MTT based *in vitro* tests on the human renal cancer cell line Caki-1 and human breast cancer cell line MCF-7 in order to determine their IC_{50} values.

The NHC–silver complexes **2a–e** were found to have IC_{50} values of 3.0 (±0.6), 0.51 (±0.07), 4.2 (±1.2), 9.0 (±0.6), 26 (±2) μM, against the renal cancer cell-line Caki-1 and IC_{50} values of 2.3 (±0.4), 1.4 (±0.2), 3.0 (±0.5), 3.4 (±1.2) and 14 (±2) μM against the breast cancer cell line MCF-7, respectively. Compared to our lead compound **SBC3** (1,3-bisbenzyl-4,5-bisphenyl-imidazole-2-ylium silver(I) acetate) (IC_{50} value = 14 (±1) μM against Caki-1 and 5.8 (±0.6) μM against MCF-7) these values represent improved cytotoxicity against both cell lines, especially for the silver complexes **2a** and **2b**. These two compounds are not only more active than **SBC3** but also exhibit in the case of **2b** a 7 times higher biological activity than cisplatin (IC_{50} value = 3.3 μM) against Caki-1.

© 2012 Elsevier B.V. All rights reserved.

1. Introduction

In the treatment of cancer, platinum-based drugs such as cisplatin, oxaliplatin and carboplatin are widely used, but due to several factors resistance against these drugs may develop during treatment. To overcome resistance many groups focus on the design of novel platinum based complexes [1] by using specific carriers, or a change from platinum to other transition metals. Novel carrier ligands must initially meet certain criteria, such as being easily accessible in few steps, substituents can be widely varied and their reactivity in biological medium can be easily fine-tuned. All these criteria are met by *N*-heterocyclic carbenes (NHCs), which are nowadays not only used in organometallic chemistry and catalysis, but more and more also in the design and synthesis of cytotoxic and antibacterial transition metal complexes. Most commonly used transition metals in the development of new anticancer and antibacterial drugs are platinum, palladium, rhodium, ruthenium, copper, silver and gold [2–15].

Silver salts such as silver nitrate are used for many years as antimicrobial agents and have exhibited low toxicity for humans, but recently an increased number of research groups focuses on the activity of new silver therapeutics as anticancer agents [4,11]. Youngs and co-workers have reported anticancer activity of NHC–silver complexes derived from 4,5-dichloro-1H-imidazole against the human cancer cell lines OVCAR-3 (ovarian), MB157 (breast), and HeLa (cervical). Activity was even demonstrated *in vivo* for [4,5-dichloro-1,3-dimethylimidazol-2-ylidene] silver(I)

* Corresponding author.
E-mail address: matthias.tacke@ucd.ie (M. Tacke).

0020-1693/$ - see front matter © 2012 Elsevier B.V. All rights reserved.
http://dx.doi.org/10.1016/j.ica.2012.10.029

acetate against an ovarian cancer xenograft model [10]. The groups of Gautier and Morel reported an *N*,*N*′-diaryl-substituted carbene of high lipophilicity as suitable ligand for metal complexes. The cytotoxicity of the resulting silver complex was 40-fold (MCF-7 and HL60) to 7-fold (MCF-7R) higher than that of cisplatin [6]. Also Gust et al. have recently reported that symmetrically and unsymmetrically substituted NHC–silver(I) halides show promising activity against different cancer cell lines as well as bacteria strains [16], which correlates well with the findings in our group [17–26].

Within this paper we present a new series of symmetrically *p*-benzyl-substituted *N*-heterocyclic carbene silver acetate complexes derived from 4,5-ditolyl-imidazole, their synthesis, cytotoxicity, and antibacterial studies.

2. Experimental part

2.1. General conditions

All silver(I) acetate reactions were carried out under exclusion of light. All solvents used were of analytical grade and were used without further purification. 4,4-Dimethylbenzoin, formamide, benzyl bromide, 4-methylbenzyl bromide, 4-methoxybenzyl chloride, methyl 4-(bromomethyl)benzoate, 4-(bromomethyl) benzonitrile, silver(I) acetate and K_2CO_3 were purchased from Sigma–Aldrich Chemical Company and were used without further purification.

^{1}H NMR spectra were measured on a Varian 300 MHz spectrometer while ^{13}C spectra were measured on a Varian 400 MHz spectrometer. All chemical shifts are reported in ppm and referenced to TMS. IR spectra were recorded on a Perkin-Elmer Paragon 1000 FT-IR spectrometer employing a KBr disc. ESI MS was performed on a quadrupole tandem mass spectrometer (Quattro Micro, Micromass/Water's Corp., USA), using solutions in 100% methanol. MS spectra were obtained in the ES+ (electron spray positive ionisation) mode for all compounds. CHN Analysis was carried out in an Exeter Analytical CE-440 elemental analyzer. Crystal Data was collected using an Agilent Technologies (former Oxford Diffraction) SuperNova diffractometer fitted with an Atlas detector. A suitable crystal of **2a** was grown from a saturated solution of diethyl ether and slow evaporation of the solvent while crystals of **2e** were grown in a saturated dichloromethane solution with slow infusion of pentane. **2a** and **2e** were measured with Mo Kα (0.71073 A°) at 100 K. A five-time redundant (**2a**) or a complete (**2e**) dataset was collected, assuming that the Friedel pairs are not equivalent. An analytical absorption correction based on the shape of the crystal was performed [27]. The structure was solved by direct methods using SHELXS-97 [28] and refined by full matrix least-squares on F^2 for all data using SHELXL-97 [28]. Hydrogen atoms were added at calculated positions and refined using a riding model. Their isotropic thermal displacement parameters were fixed to 1.2 (1.5 for methyl groups) times the equivalent ones of the parent atom. Anisotropic thermal displacement parameters were used for all non hydrogen atoms.

2.2. Synthesis

2.2.1. Synthesis of 4,5-bis(4-methylphenyl)-1H-imidazole (**1**)

4,5-Bis(4-methylphenyl)-1H-imidazole was synthesised according to literature [29] to give a yield of 66%. The formation of the product was confirmed by NMR.

2.2.2. Synthesis of 1,3-bis-benzyl-4,5-bis-(4-methylphenyl)-imidazolium bromide (**1a**)

4,5-Bis-(4-methylphenyl)-1H-imidazole (248 mg, 1.00 mmol), 2 equivalents of benzyl bromide (0.24 mL, 2.00 mmol) and 1.5 equivalents of K_2CO_3 (207 mg, 1.50 mmol) were dissolved in acetonitrile and stirred for 2 d at room temperature. After filtering off the precipitate and removing the solvent under reduced pressure the obtained sticky white solid was washed with pentane (2 × 20 mL) and diethyl ether (2 × 20 mL) to yield a white powder (280 mg, 0.55 mmol, 55% yield).

^{1}H NMR (δ ppm, DMSO, 400 MHz): 9.57 (s, 1H, NCHN), 7.28–7.26 (m, 4H), 7.16–7.12 (m, 8H), 6.99–6.96 (m, 6H), 5.37 (s, 4H, CH_2), 2.26 (s, 6H, CH_3).

^{13}C NMR (δ ppm, DMSO, 101 MHz): 140.28 (NCHN), 136.82, 134.63, 132.25, 131.10, 129.83, 129.27, 128.93, 128.17, 122.47 (C_{benzyl} + C_{tolyl} + $C_{imidazole}$), 50.82 (CH_2), 21.30 (CH_3).

IR absorptions (KBr, cm^{-1}): 3421 (m), 3031 (s), 2942 (s), 1619 (s), 1558 (s), 1502 (s), 1452 (s), 817 (s).

MS (*m*/*z*, QMS-MS/MS): 509.00 [M$^+$−H].

Micro *Anal.* Calc. for $C_{31}H_{29}BrN_2$ (509.48): C, 73.08; H, 5.74; N, 5.50. Found: C, 72.37, H 5.52, N 5.41%.

Melting point: 203–206 °C

2.2.3. Synthesis of 1,3-bis-(4-methylbenzyl)-4,5-bis-(4-methylphenyl)-imidazolium bromide (**1b**)

4,5-Bis-(4-methylphenyl)-1H-imidazole (248 mg, 1.00 mmol), 2 equivalents of 4-methylbenzyl bromide (371 mg, 2.00 mmol) and 1.5 equivalents of K_2CO_3 (207 mg, 1.50 mmol) were dissolved in acetonitrile and stirred for 2 d at room temperature. After filtering off the precipitate and removing the solvent under reduced pressure the obtained sticky white solid was washed with pentane (2 × 20 mL) and diethyl ether (2 × 20 mL) to yield a white powder (200 mg, 0.37 mmol, 37% yield).

^{1}H NMR (δ ppm, $CDCl_3$, 300 MHz): 11.07 (s, 1H, NCHN), 7.14 (d, *J* = 7.7 Hz, 4H), 7.10–7.00 (m, 8H), 6.97 (d, *J* = 7.8 Hz, 4H), 5.41 (s, 4H, CH_2), 2.35 (s, 6H, CH_{3tolyl}), 2.30 (s, 6H, $CH_{3benzyl}$).

^{13}C NMR (δ ppm, $CDCl_3$, 101 MHz): 140.60 (NCHN), 138.86, 136.96, 132.01, 130.64, 130.54, 129.73, 129.70, 128.48, 121.86 ($C_{methylbenzyl}$ + C_{tolyl} + $C_{imidazole}$), 50.96 (CH_2), 21.39 (CH_{3tolyl}), 21.16 ($CH_{3benzyl}$).

IR absorptions (KBr, cm^{-1}): 3423 (m), 3010 (s), 2865 (s), 1558 (s), 1515 (s), 1450 (s), 817 (s)

MS (*m*/*z*, QMS-MS/MS): 457.64 [M$^+$−Br].

Micro *Anal.* Calc. for $C_{33}H_{33}BrN_2$ (537.53): C, 73.74; H, 6.19; N, 5.21. Found: C, 73.44; H, 6.12; N, 5.01%.

Melting point: 212–214 °C.

2.2.4. Synthesis of 1,3-bis-(4-methoxybenzyl)-4,5-bis-(4-methylphenyl)-imidazolium chloride (**1c**)

4,5-Bis-(4-methylphenyl)-1H-imidazole (248 mg, 1.00 mmol), 2 equivalents of 4-methoxybenzyl chloride (0.24 mL, 2.00 mmol) and 1.5 equivalents of K_2CO_3 (207 mg, 1.50 mmol) were dissolved in acetonitrile and refluxed for 3 d. After filtering off the precipitate and removing the solvent under reduced pressure the obtained sticky white solid was washed with pentane (2 × 20 mL) and diethyl ether (2 × 20 mL) to yield a white powder (200 mg, 0.38 mmol, 38% yield).

^{1}H NMR (δ ppm, $CDCl_3$, 300 MHz): 11.57 (s, 1H, NCHN), 7.12 (dd, *J* = 15.7, 8.2 Hz, 8H), 6.95 (d, *J* = 8.1 Hz, 4H), 6.77 (d, *J* = 8.7 Hz, 4H), 5.39 (s, 4H, CH_2), 3.76 (s, 6H, OCH_3), 2.36 (s, 6H, CH_3).

^{13}C NMR (δ ppm, $CDCl_3$, 101 MHz): 159.90 (NCHN), 140.56, 131.69, 130.62, 130.27, 129.74, 128.45, 125.75, 122.00, 114.29, ($C_{methoxybenzyl}$ + C_{tolyl} + $C_{imidazole}$) 55.25 (CH_2), 50.67 (OCH_3), 21.39 (CH_3).

IR absorptions (KBr, cm^{-1}): 3421 (m), 3088–2956 (m), 1613 (s), 1514 (s), 1452 (s), 1250 (s), 1178 (s), 821 (s).

MS (*m*/*z*, QMS-MS/MS): 489.49 [M$^+$−HCl].

Micro *Anal.* Calc. for $C_{33}H_{33}ClN_2O_2$ (525.08): C, 75.48; H, 6.33; N, 5.34. Found: C, 75.28; H, 6.22; N, 5.13%.

Melting point: 196–198 °C.

*2.2.5. Synthesis of 1,3-bis-(4-methoxycarbonylbenzyl)-4,5-bis-(4-methylphenyl)-imidazolium bromide (**1d**)*

4,5-Bis-(4-methylphenyl)-1H-imidazole (248 mg, 1.00 mmol), 2 equivalents of 4-methoxycarbonylbenzyl bromide (458 mg, 2.00 mmol) and 1.5 equivalents of K_2CO_3 (207 mg, 1.50 mmol) were dissolved in acetonitrile and stirred for 3 d at room temperature. After filtering off the precipitate and removing the solvent under reduced pressure the obtained sticky white solid was washed with pentane (2 × 20 mL) and diethyl ether (2 × 20 mL) to yield a white powder (100 mg, 0.16 mmol, 16% yield).

^{1}H NMR (δ ppm, DMSO, 400 MHz): 9.57 (s, 1H, NCHN), 7.89 (d, J = 8.4 Hz, 4H), 7.25 (d, J = 8.1 Hz, 4H), 7.14 (s, 8H), 5.49 (s, 4H, CH_2), 3.83 (s, 6H, CH_3), 2.24 (s, 6H, CH_{3tolyl}).

^{13}C NMR (δ ppm, DMSO, 101 MHz): 166.19 (C═O), 140.37 (NCHN), 139.83, 132.39, 131.04, 129.96, 129.82, 128.92, 128.38, 124.98, 122.26 ($C_{methoxycarbonylbenzyl}$ + C_{phenyl} + $C_{imidazole}$), 52.74 (CH_2), 50.55 (OCH_3), 21.28 (CH_{3tolyl}).

IR absorptions (KBr, cm^{-1}): 3423 (m), 2950 (s), 1722 (s), 1614 (s), 1434 (s), 1280 (s), 821 (s).

MS (*m*/*z*, QMS-MS/MS): 545.54 [M$^+$−Br].

Micro *Anal.* Calc. for $C_{35}H_{33}BrN_2O_4$ (625.55): C, 67.20; H, 5.32; N, 4.48. Found: C, 67.10; H, 5.20; N, 4.80%.

Melting point: 207–211 °C.

*2.2.6. Synthesis of 1,3-bis-(4-cyanobenzyl)-4,5-bis-(4-methylphenyl)-imidazolium bromide (**1e**)*

4,5-Bis-(4-methylphenyl)-1H-imidazole (248 mg, 1.00 mmol), 2 equivalents of 4-cyanobenzyl bromide (391 mg, 2.00 mmol) and 1.5 equivalents of K_2CO_3 (207 mg, 1.50 mmol) were dissolved in acetonitrile and stirred for 2 d at room temperature. After filtering off the precipitate and removing the solvent under reduced pressure the obtained sticky white solid was washed with pentane (2 × 20 mL) and diethyl ether (2 × 20 mL) to yield a white powder (327 mg, 0.58 mmol, 58% yield).

^{1}H NMR (δ ppm, DMSO, 400 MHz): 9.57 (s, 1H, NCHN), 7.81 (d, J = 8.3 Hz, 4H), 7.32 (d, J = 8.4 Hz, 4H), 7.13 (s, 8H), 5.50 (s, 4H, CH_2), 2.24 (s, 6H, CH_3).

^{13}C NMR (δ ppm, DMSO, 101 MHz): 140.39 (NCHN), 140.02 (CN), 137.51, 133.06, 132.32, 131.02, 129.82, 129.06, 122.21, 118.86, 111.57 ($C_{cyanobenzyl}$ + C_{tolyl} + $C_{imidazole}$), 50.47 (CH_2), 21.29 (CH_3).

IR absorptions (KBr, cm^{-1}): 3461 (m), 2966 (m), 2227 (s), 1614 (s), 1560 (s), 1448 (s), 821 (s).

MS (*m*/*z*, QMS-MS/MS): 479.57 [M$^+$−HBr].

Micro *Anal.* Calc. for $C_{33}H_{27}BrN_4$ (559.50): C, 70.84; H, 4.86; N, 10.01. Found: C, 70.56; H, 4.62; N, 9.85%.

Melting point: 279–281 °C.

*2.2.7. Synthesis of 1,3-bis-benzyl-4,5-bis-(4-methylphenyl)-imidazole-2-ylidene silver(I) acetate (**2a**)*

1,3-Bis-benzyl-4,5-bis-(4-methylphenyl)-imidazolium bromide (**1a**) (100 mg, 0.19 mmol) and 2.1 equivalents of silver(I) acetate (69 mg, 0.41 mmol) were dissolved in 30 mL of dichloromethane and stirred in darkness at room temperature for 2 d. After filtering off the AgBr by-product, the solvent was reduced to 3 mL and by adding dropwise 10 mL of pentane a white powder precipitated. The solvent was decanted and the white precipitate was washed with pentane (2 × 10 mL) and diethyl ether (3 × 10 mL) to yield a white powder (90 mg, 0.15 mmol, 77% yield).

^{1}H NMR (δ ppm, $CDCl_3$, 300 MHz): 7.25–7.20 (m, 6H), 7.02 (d, J = 7.9 Hz, 8H), 6.87 (d, J = 7.9 Hz, 4H), 5.30 (s, 4H, CH_2), 2.29 (s, 6H, CH_{3tolyl}), 2.07 (s, 3H, $CH_{3acetate}$).

^{13}C NMR (δ ppm, $CDCl_3$, 101 MHz): 198.98 (NCN), 164.32 (C═O), 138.07, 135.40, 129.48, 128.93, 128.23, 127.62, 126.91, 126.34, 124.76, 123.81 (C_{tolyl} + $C_{imidazole}$ + C_{benzyl}), 52.51 (CH_2), 20.27 (CH_{3tolyl})

IR absorptions (KBr, cm^{-1}): 3480–3416 (m), 2360 (s), 1598 (s), 1440 (s), 1375 (s), 1020 (s), 817 (s).

MS (*m*/*z*, QMS-MS/MS): 429.61 [M$^+$−AgOAc].

Micro *Anal.* Calc. for $C_{33}H_{32}AgN_2O_2$ (596.49): C, 66.45; H, 5.41; N, 4.70. Found: C, 66.44; H, 5.39; N, 4.54%.

Melting point: 143–147 °C.

*2.2.8. Synthesis of 1,3-bis-(4-methylbenzyl)-4,5-bis-(4-methylphenyl)-imidazole-2-ylidene silver(I) acetate (**2b**)*

1,3-Bis-(4-methylbenzyl)-4,5-bis-(4-methylphenyl)-imidazolium bromide (**1b**) (100 mg, 0.19 mmol) and 2 equivalents of silver(I) acetate (65 mg, 0.39 mmol) were dissolved in 30 mL of dichloromethane and stirred in darkness at room temperature for 2 d. After filtering off the AgBr by-product, the solvent was reduced to 3 mL and by adding dropwise 10 mL of pentane a white powder precipitated. The solvent was decanted and the white precipitate was washed with pentane (2 × 10 mL) and diethyl ether (3 × 10 mL) to yield a white powder (90 mg, 0.14 mmol, 78% yield).

^{1}H NMR (δ ppm, $CDCl_3$, 300 MHz): 7.91 (d, J = 8.0 Hz, 4H, CH_{benzyl} + CH_{tolyl}), 7.04 (t, J = 8.0 Hz, 8H, CH_{benzyl} + CH_{tolyl}), 6.85 (d, J = 8.0 Hz, 4H, CH_{benzyl} + CH_{tolyl}), 5.37 (s, 4H, CH_2), 3.90 (s, 6H, $CH_{3benzyl}$), 2.29 (s, 6H,CH_{3tolyl}), 2.06 (s, 1H, $CH_{3actetate}$).

^{13}C NMR (δ ppm, $CDCl_3$, 101 MHz): 177.16 (NCN), 138.97 (C═O), 137.60, 133.47, 132.38, 130.52, 129.53, 129.27, 129.22, 128.26, 127.37, 124.95 (CH_{tolyl} + CH_{benzyl} + $CH_{imidazole}$), 53.19 (CH_2), 21.27 (CH_3), 21.09 (CH_3).

IR absorptions (KBr, cm^{-1}): 3437 (m), 3028 (s), 2921 (s), 1708 (s), 1517 (s), 819 (s)

MS (*m*/*z*, QMS-MS/MS): 451.53 [M$^+$−AgOAc].

Micro *Anal.* Calc. for $C_{35}H_{36}AgN_2O_2$ (624.54): C, 67.31; H, 5.81; N, 4.49. Found: C, 66.98; H, 5.53; N, 4.09%.

Melting point: 126–128 °C.

*2.2.9. Synthesis of 1,3-bis-(4-methoxybenzyl)-4,5-bis-(4-methylphenyl)-imidazole-2-ylidene silver(I) acetate (**2c**)*

1,3-Bis-(4-methoxybenzyl)-4,5-bis-(4-methylphenyl)-imidazolium chloride (**1c**) (100 mg, 0.18 mmol) and 2.1 equivalents of silver(I) acetate (62 mg, 0.38 mmol) were dissolved in 30 mL of dichloromethane and stirred in darkness at room temperature for 2 d. After filtering off the AgBr by-product, the solvent was reduced to 3 mL and by adding dropwise 10 mL of pentane a white powder precipitated. The solvent was decanted and the white precipitate was washed with pentane (2 × 10 mL) and diethyl ether (3 × 10 mL) to yield a white powder (70 mg, 0.10 mmol, 56% yield).

^{1}H NMR (δ ppm, $CDCl_3$, 300 MHz): 7.05 (d, J = 8.0 Hz, 4H), 6.91 (m, 8H), 6.74 (d, J = 8.0 Hz, 4H), 5.22 (s, 4H, CH_2), 3.76 (s, 6H, $CH_{3methoxybenzyl}$), 2.31 (s, 6H, CH_{3tolyl}), 2.09 (s, 3H, $CH_{3acetate}$).

^{13}C NMR (δ ppm, $CDCl_3$, 101 MHz): 178.62 (NCN), 159.21 (C═O), 138.99, 132.31, 130.54, 129.23, 128.95, 128.51, 124.98, 123.56, 113.95 ($C_{methoxybenzyl}$ + C_{tolyl} + $C_{imidazole}$), 55.23 (CH_2), 52.98 (OCH_3), 22.81 (CH_{3tolyl}), 21.28 ($CH_{3acetate}$).

IR absorptions (KBr, cm^{-1}): 3398 (m), 3003 (s), 2920 (s), 1576 (s), 1513 (s), 1384 (s), 1252 (s), 820 (s).

MS (*m*/*z*, QMS-MS/MS): 489.52 [M$^+$−AgOAc].

Micro *Anal.* Calc. for $C_{35}H_{36}AgN_2O_4$ (656.54): C, 64.03; H, 5.53; N, 4.27. Found: C, 63.41; H, 5.28; N, 4.03%.

Melting point: 166–168 °C.

*2.2.10. Synthesis of 1,3-bis-(4-methoxycarbonylbenzyl)-4,5-bis-(4-methylphenyl)-imidazole-2-ylidene silver(I) acetate (**2d**)*

1,3-Bis-(4-methoxycarbonylbenzyl)-4,5-bis-(4-methylphenyl)-imidazolium bromide (**1d**) (100 mg, 0.16 mmol) and 2 equivalents of silver(I) acetate (56 mg, 0.33 mmol) were dissolved in 30 mL of dichloromethane and stirred in darkness at room temperature for 2 d. After filtering off the AgBr by-product, the solvent was reduced to 3 mL and by adding dropwise 10 mL of pentane a white powder

precipitated. The solvent was decanted and the white precipitate was washed with pentane (2 × 10 mL) and diethyl ether (3 × 10 mL) to yield a white powder (60 mg, 0.08 mmol, 53% yield).

^{1}H NMR (δ ppm, $CDCl_3$, 300 MHz): 7.91 (d, J = 8.0 Hz, 4H), 7.04 (t, J = 8.3 Hz, 8H), 6.85 (d, J = 8.0 Hz, 4H), 5.37 (s, 4H, CH_2), 3.91 (s, 6H, $CH_{3methoxycarbonylbenzyl}$), 2.29 (s, 6H, CH_{3tolyl}), 2.06 (s, 3H, $CH_{3acetate}$).

^{13}C NMR (δ ppm, $CDCl_3$, 101 MHz): 179.13 (NCN), 169.67 (C=O), 166.56 (C=O), 141.15, 139.45, 132.75, 130.34, 129.99, 129.87, 129.40, 127.20, 124.31, 53.29 (CH_2), 52.16 (OCH_3), 22.79 ($CH_{3acetate}$), 21.27 (CH_{3tolyl}).

IR absorptions (KBr, cm^{-1}): 3434 (m), 2950 (w), 1724 (s), 1579 (m), 1434 (m), 819 (s).

MS (m/z, QMS-MS/MS): 547.45 [M^+−AgOAc].

Micro *Anal.* Calc. for $C_{37}H_{36}AgN_2O_6$ (712.56): C, 62.37; H, 5.09; N, 3.93. Found: C, 61.66; H, 4.78; N, 3.72%.

Melting point: 196–198 °C.

2.2.11. Synthesis of 1,3-bis-(4-cyanobenzyl)-4,5-bis-(4-methylphenyl)-imidazole-2-ylidene silver(I) acetate (**2e**)

1,3-Bis-(4-cyanobenzyl)-4,5-bis-(4-methylphenyl)-imidazolium bromide (**1e**) (100 mg, 0.18 mmol) and 2.1 equivalents of silver(I) acetate (63 mg, 0.37 mmol) were dissolved in 30 mL of dichloromethane and stirred in darkness at room temperature for 2 d. After filtering off the AgBr by-product, the solvent was reduced to 3 mL and by adding dropwise 10 mL of pentane a white powder precipitated. The solvent was decanted and the white precipitate was washed with pentane (2 × 10 mL) and diethyl ether (3 × 10 mL) to yield a white powder (104 mg, 0.16 mmol, 90% yield).

^{1}H NMR (δ ppm, $CDCl_3$, 300 MHz): 7.53 (d, J = 7.9 Hz, 4H), 7.08 (dd, J = 11.0, 8.0 Hz, 8H), 6.86 (d, J = 7.9 Hz, 4H), 5.37 (s, 4H, CH_2), 2.31 (s, 6H, CH_{3tolyl}), 2.06 (s, 3H, $CH_{3acetate}$).

^{13}C NMR (δ ppm, $CDCl_3$, 101 MHz): 179.13 (NCN), 165.98 (C=O), 141.04 (CN), 139.84, 132.80, 132.53, 130.24, 129.59, 128.12, 123.96, 118.24, 112.20 ($C_{cyanobenzyl} + C_{tolyl} + C_{imidazole}$), 53.15 ($CH_2$), 22.70 ($CH_{3tolyl}$), 21.29 ($CH_{3acetate}$).

IR absorptions (KBr, cm^{-1}): 3430 (s), 2925 (w), 2227 (m), 1581 (s), 1506 (m), 1405 (s), 819 (m).

MS (m/z, QMS-MS/MS): 479.44 [M^+−AgOAc].

Micro *Anal.* Calc. for $C_{35}H_{30}AgN_4O_2$ (646.51): C, 65.02; H, 4.68; N, 8.67. Found: C, 64.82; H, 4.37; N, 8.28%.

Melting point: 161–163 °C.

2.3. Antibacterial studies

The silver(I) acetate complexes were screened in preliminary *in vitro* antibacterial tests against two bacterial strains. The test organisms included *Staphylococcus aureus* (SA) (NCTC 7447) as a Gram-positive bacteria and *Escherichia coli* (*E. coli*) as Gram-negative bacteria.

To assess the biological activity of compounds **2a**–**e** the qualitative Kirby–Bauer disk-diffusion method was applied [30]. All bacteria were individually cultured from a single colony in sterile LB medium [31] overnight at 37 °C in an orbital shaker incubator. All the work carried out was performed under sterile conditions.

For each strain, 70 μL of culture were spread evenly on agar-LB medium. Four 5 mm diameter Whatman paper discs were placed evenly separated on each plate. Two stock solutions (9:1 DMSO:H_2O) of every compound were prepared at 2.2 and 4.4 μM to be able to test the effect of different concentrations. Each plate was then tested with 5 and 7 μL of 2.2 μM solution and 5 and 10 μL for the 4.4 μM solution. The plates were covered and placed in an incubator at 37 °C for 24 h. The plates were then removed and the area of clearance, which is defined as the distance between the edge of the filter paper disc and the beginning of the bacterial growth, was measured for each sample in mm.

2.4. Cytotoxicity studies

Preliminary *in vitro* cell tests were performed on the human cancerous renal cell line Caki-1 in order to compare the cytotoxicity of the compounds presented in this paper. This cell line was chosen based on its regular and long-lasting growth behaviour, which is similar to the one shown in kidney carcinoma cells. The cells were obtained from the ATCC (American Tissue Cell Culture Collection) and maintained in Dulbecco's Modified Eagle Medium containing 10% (v/v) FCS (fetal calf serum), 1% (v/v) penicillin streptomycin and 1% (v/v) L-glutamine. Cells were seeded in 96-well plates containing 200 μL microtitre wells at a density of 5000-cells/200 μL of medium and were incubated at 37 °C for 24 h to allow for exponential growth. Then the compounds used for the testing were dissolved in the minimal amount of DMSO (dimethylsulfoxide) possible and diluted with medium to obtain stock solutions of 5×10^{-4} M in concentration and less than 0.7% of DMSO. The cells were then treated with varying concentrations of the compounds and incubated for 48 h at 37 °C. Then, the solutions were removed from the wells and the cells were washed with PBS (phosphate buffer solution) and fresh medium was added to the wells. Following a recovery period of 24 h incubation at 37 °C, individual wells were treated with 200 μL of a solution of MTT (3-(4,5-dimethylthiazol-2-yl)-2,5-diphenyltetrazolium bromide) in medium. The solution consisted of 22 mg of MTT in 40 mL of medium. The cells were incubated for 3 h at 37 °C. The medium was then removed and the purple formazan crystals were dissolved in 200 μL DMSO per well. For all tests cells with low passage numbers were used. A Wallac Victor (Multilabel HTS Counter) Plate Reader was used to measure absorbance at 540 nm. Cell viability was expressed as a percentage of the absorbance recorded for control wells. The values used for the dose response curves represent the values obtained from four consistent MTT-based assays for each compound tested.

3. Results and discussion

3.1. Synthesis

The synthetic route for symmetrically substituted imidazole starting materials, *N*-heterocyclic carbenes as ligand precursors and their corresponding silver complexes described in here is given in Scheme 1. The initial symmetrically 4,5-diaryl-substituted imidazole starting material was prepared by reacting 2-bis(4-methylphenyl)ethane-1,2-dione with formamide to form 4,5-bis(4-methylphenyl)-1H-imidazole (**1**) according to literature [29], with 60% yield.

The symmetrically substituted NHC precursors 1,3-bis-benzyl-4,5-bis-(4-methylphenyl)-imidazolium bromide (**1a**), 1,3-bis-(4-methylbenzyl)-4,5-bis-(4-methylphenyl)-imidazolium bromide (**1b**), 1,3-bis-(4-methoxycarbonylbenzyl)-4,5-bis-(4-methylphenyl)-imidazolium bromide (**1d**) and 1,3-bis-(4-cyanobenzyl)-4,5-bis-(4-methylphenyl)-imidazolium bromide (**1e**) were prepared by stirring 4,5-bis(4-methoxylphenyl)-1H-imidazole (**1**) with 2 equivalents of appropriately *p*-substituted benzyl bromide in the presence of K_2CO_3 in acetonitrile at room temperature for 1–5 d with 35, 99, 38 and 50% yields, respectively. The symmetrically substituted NHC precursor 1,3-bis-(4-methoxybenzyl)-4,5-bis-(4-methylphenyl)-imidazolium chloride (**1c**) was synthesised by stirring 4,5-bis(4-methoxylphenyl)-1H-imidazole (**1**) with 2 equivalents of 4-methoxybenzyl chloride in the presence of K_2CO_3 in acetonitrile at 80 °C temperature for 9 d with 38% yield (ii).

The NHC precursors were characterised by spectral (^{1}H, ^{13}C NMR, IR and MS) and elemental analysis studies. The ^{1}H NMR spectra of all NHC precursors **1a**–**e** show a characteristic downfield

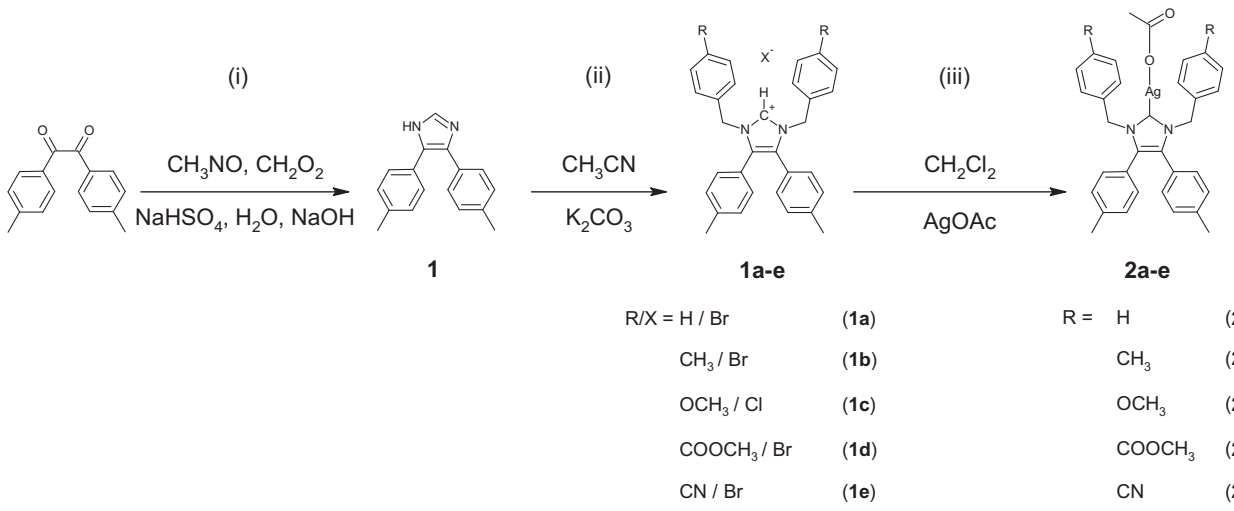

Scheme 1. General reaction scheme for the synthesis of (i) 4,5-bistolyl-imidazole (**1**), (ii) 1,3-bis-(*p*-substituted benzyl)-4,5-bistolyl imidazolium halides (**1a**–**e**) and (iii) 1,3-bis-(*p*-substituted benzyl)-4,5-bistolyl imidazole-2-ylium silver acetates (**2a**–**e**).

shift in the range d = 9.27–11.05 ppm for the NCHN proton attributable to the positive charge of the molecule [32,33] .In addition, their identities have also been confirmed by a base peak for the [M^+−Br] or [M^+−Cl] fragments in their positive mode ESI mass spectra.

The NHC–silver complexes 1,3-bis-benzyl-4,5-bis-(4-methylphenyl)-imidazole-2-ylidene silver(I) acetate (**2a**), 1,3-bis-(4-methylbenzyl)-4,5-bis-(4-methylphenyl)-imidazole-2-ylidene silver(I) acetate (**2b**), 1,3-bis-(4-methoxybenzyl)-4,5-bis-(4-methylphenyl)-imidazole-2-ylidene silver(I) acetate (**2c**), 1,3-bis-(4-methoxycarbonylbenzyl)-4,5-bis-(4-methylphenyl)-imidazole-2-ylidene silver(I) acetate (**2d**) and 1,3-bis-(4-cyanobenzyl)-4,5-bis-(4-methylphenyl)-imidazole-2-ylidene silver(I) acetate (**2e**) were synthesised by the reaction of **1a**–**e** with 2.1 equivalents of silver acetate in dichloromethane. The reaction mixture was stirred for 1–3 d at room temperature to afford the NHC–silver acetate complexes as off white solid in 77, 78, 56, 53 and 90% yields, respectively.

The complexes were characterised by spectral (^{1}H, ^{13}C NMR, IR, UV–Vis and MS) and elemental analysis studies. Furthermore, the

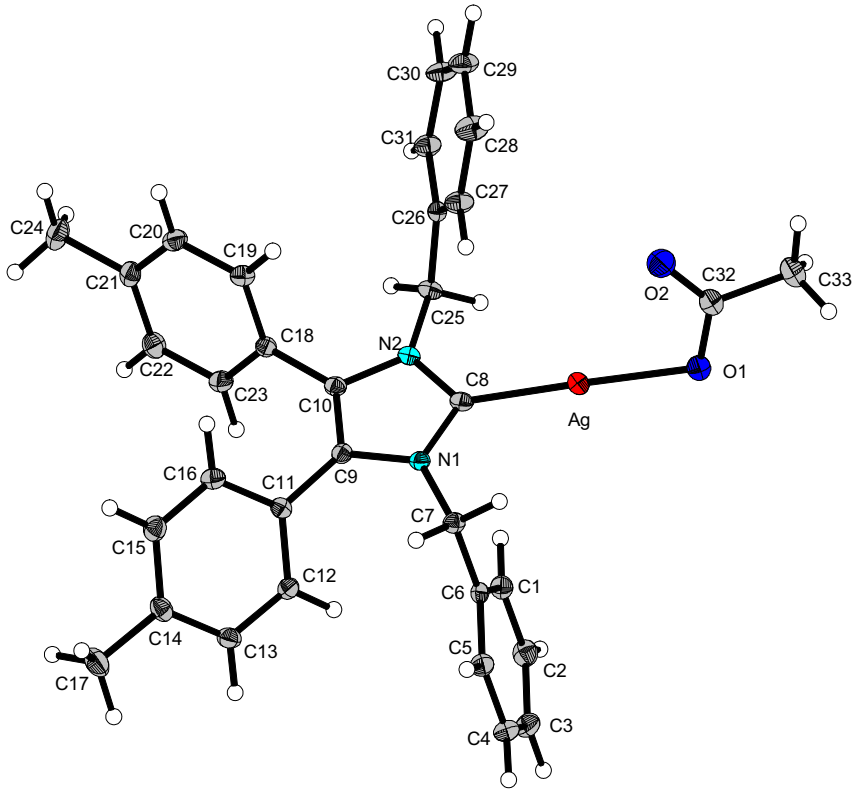

Fig. 1. X-ray diffraction structure of **2a**; thermal ellipsoids are drawn on the 50% probability level.

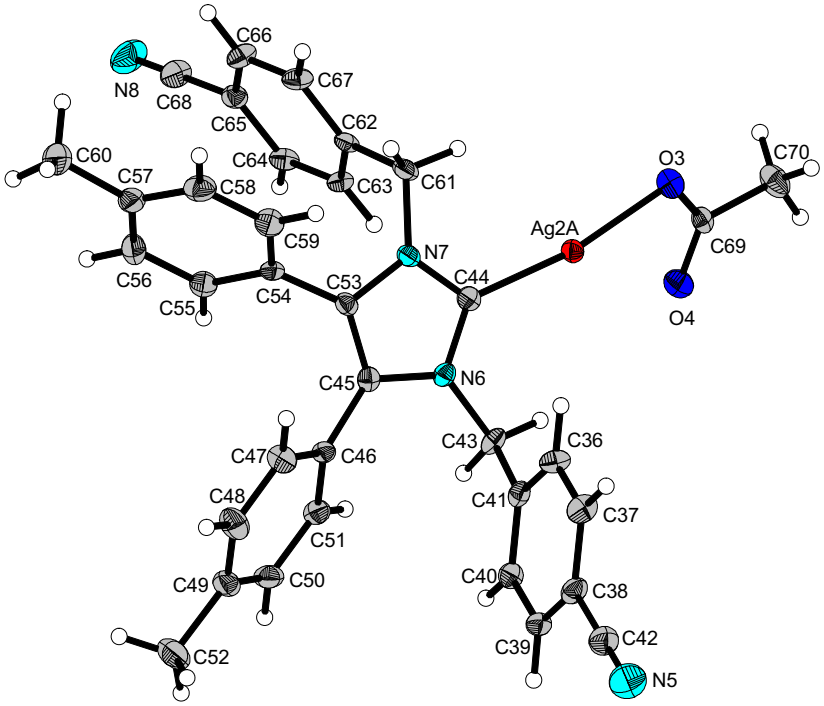

Fig. 2. X-ray diffraction structure of **2e** showing the major occupied Ag position; thermal ellipsoids are drawn on the 50% probability level.

solid state structures of **2a** and **2e** were analysed by single crystal X-ray diffraction. Absence of a downfield NCHN signal in the range between 11.57–9.57 ppm and presence of new signals at 2.09–2.06 ppm for the acetate protons in all ^{1}H NMR spectra for **2a**–**e** however, indicates a successful complex formation. The ^{13}C NMR resonances of the carbene carbon atoms in complexes **2a**–**e** occur in the range d 198.98–178.16 ppm respectively. These signals are shifted downfield compared to the corresponding precursors of **1a**–**e** carbene carbons resonance in the range of 159.90–140.28 ppm respectively, which further demonstrates the formation of the expected NHC–silver acetate complexes. Finally, positive mode ESI mass spectra of all five NHC–silver complexes (**2a**–**e**) are dominated by $[M^{+}-O_2CCH_3]$ fragment peaks arising from the loss of the acetate ligand.

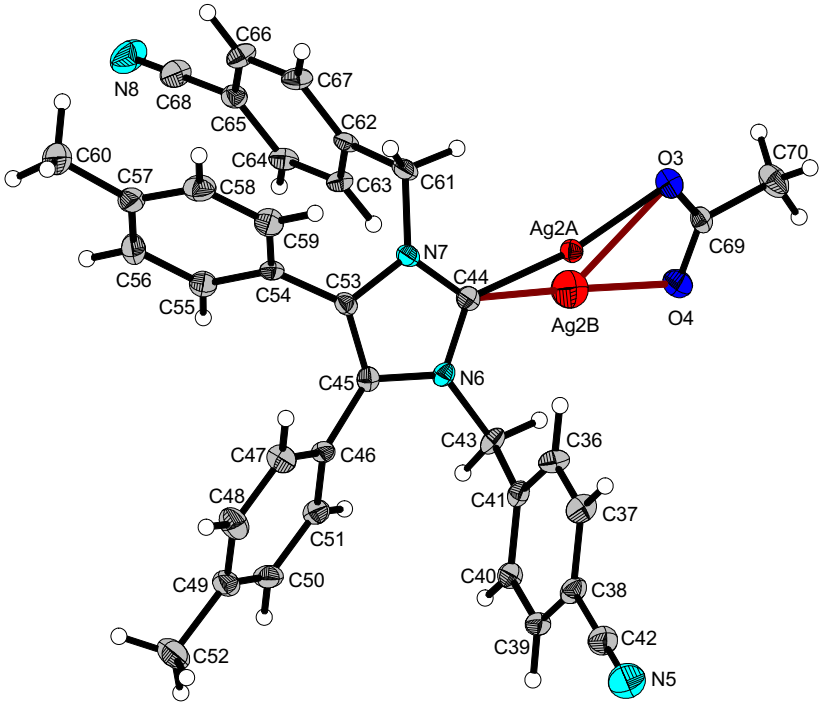

Fig. 3. X-ray diffraction structure of **2e** showing both Ag positions; thermal ellipsoids are drawn on the 50% probability level, Ag2B with fixed radius.

Table 1
Crystal data and structure refinement for complexes **2a** and **2e**.

	2a	**2e**
Empirical formula	$C_{33}H_{32}N_2O_2Ag$	$C_{35}H_{29}N_4O_2Ag$
Formula weight (g/mol)	595.47	645.49
Crystal system	monoclinic	triclinic
Space group	$P2_1/c$ (#14)	$P\bar{1}$ (#2)
Unit cell dimensions		
a (Å)	12.1787(1)	7.8609(1)
b (Å)	8.77455(7)	16.5810(3)
c (Å)	25.4346	23.7243(4)
α (°)		89.668(2)
β (°)	98.4644(8)	89.978(1)
γ (°)		89.995(1)
V (Å^3)	2688.40(4)	3092.21(9)
Z	4	4
Density (mg/m^3) (calc.)	1.471	1.387
Absorption coefficient (mm$^{-1)}$	0.783	0.689
F(000)	1224	1320
Crystal size (mm^3)	0.2205 × 0.1377 × 0.0790	0.2042 × 0.1250 × 0.0356
θ (°)	2.83–29.36	2.99–26.41
Index ranges	$-16 \leqslant h \leqslant 16$ $-11 \leqslant k \leqslant 12$ $-34 \leqslant l \leqslant 34$	$-9 \leqslant h \leqslant 9$ $-20 \leqslant k \leqslant 20$ $-29 \leqslant l \leqslant 29$
Reflections collected	58286	52284
Independent reflections R_{int}	7058 (0.0314)	12634 (0.0427)
Completeness to θ_{max} (%)	95.6	99.6
Maximum and minimum transmission	0.949 and 0.891	0.976 and 0.905
Data/restraints/parameters	7058/0/346	12634/0/769
Goodness-of-fit (GOF) on F^2	1.094	1.063
Final R indices [$I > 2\sigma(I)$]	R_1 = 0.0264	R_1 = 0.0254
	wR_2 = 0.0645	wR_2 = 0.0542
R Indices (all data)	R_1 = 0.0318	R_1 = 0.0294
	wR_2 = 0.0676	wR_2 = 0.0561
Largest difference in peak and hole (e Å^{-3})	0.516 and −0.472	0.596 and −0.501

3.2. Structural discussion

Suitable crystals for X-ray crystallography to determine the molecular structure of **2a** were formed from a saturated solution of diethyl ether and slow evaporation of the solvent. **2e** was grown from a saturated solution of chloroform with slow infusion of pentane.

Compound **2a** crystallises in the monoclinic space group $P21/c$ (#14) while **2e** crystallised in the triclinic space group $P\bar{1}$ (#2). Both compounds **2a** and **2e** crystallise with 4 molecules in the unit cell. The molecular structures of the compounds **2a** and **2e** are shown in Figs. 1–3. The crystal data and refinement details for the compounds mentioned above are tabulated in Table 1, while selected bond lengths and bond angles are compiled in Tables 2 (**2a**) and 3 (**2e**).

The NHC–silver complexes **2a** and **2e** are mononuclear complexes. In the NHC–silver complex **2a** (Fig. 1) the bond lengths and bond angles within the ligand agree with literature data for complexes of related ligands [34–38]. Complex **2e** shows two independent molecules in the unit cell, which are shown in Figs. 2 and 3. Selected bond lengths (Å) and bond angles (°) for both types of species for complex **2e** are shown in Table 3.

Table 2
Selected bond lengths (Å) and bond angles (°) for complexes **2a** and **2e.**

2a	Bond length (Å)	**2e**	Bond length (Å)
Ag–C(8)	2.0548(17)	Ag(1)–C(9)	2.057(2)
Ag–O(1)	2.1100(13)	Ag(1)–O(1)	2.1101(16)
N(1)–C(8)	1.354(2)	N(2)–C(9)	1.356(3)
N(1)–C(9)	1.397(2)	N(2)–C(10)	1.396(3)
C(8)-N(2)	1.355(2)	C(9)–N(3)	1.348(3)
C(10)–N(2)	1.392(2)	C(10)–C(18)	1.365(3)
C(9)–C(10)	1.363(2)	C(18)–N(3)	1.391(3)
		C(9)–Ag(1)–O(1)	176.66(9)
		N(3)–C(9)–N(2)	104.6(2)
		N(2)–C(9)–Ag(1)	127.33(17)
2a	Bond angle (°)	**2e**	Bond angle (°)
C(8)–Ag–O(1)	178.18(6)	C(9)–Ag(1)–O(1)	176.66(9)
N(1)–C(8)–N(2)	104.76(14)	N(3)–C(9)–N(2)	104.6(2)
N(1)–C(8)–Ag	128.30(12)	N(2)–C(9)–Ag(1)	127.33(17)
N(2)–C(8)–Ag	126.93(12)	N(3)–C(9)–Ag(1)	128.00(18)
C(10)–C(9)–N(1)	106.01(14)	C(18)–C(10)–N(2)	105.8(2)
C(9)–C(10)–N(2)	106.59(14)	C(10)–C(18)–N(3)	106.5(2)
C(8)–N(2)–C(10)	111.24(14)	C(9)–N(2)–C(10)	111.50(19)
C(32)–O(1)–Ag	107.35(11)		
O(2)–C(32)–O(1)	124.14(17)	C(34)–O(1)–Ag(1)	107.87(15)
O(2)–C(32)–C(33)	120.71(17)	O(2)–C(34)–O(1)	124.8(2)
O(1)–C(32)–C(33)	115.12(16)	O(2)–C(34)–C(35)	119.0(2)
		O(1)–C(34)–C(35)	116.2(2)

Table 3
Selected bond lengths (Å) and bond angles (°) for both types of species of complex **2e**.

2e (95% species)	Bond length (Å)	**2e** (5% species)	Bond length (Å)
Ag(2A)–C(44)	2.049(2)	Ag(2B)–C(44)	2.202(6)
Ag(2A)–O(3)	2.1103(17)	Ag(2B)–O(4)	2.274(6)
		Ag(2B)–O(3)	2.479(6)
N(6)–C(44)	1.361(3)	N(6)–C(44)	1.361(3)
N(6)–C(45)	1.402(3)	N(6)–C(45)	1.402(3)
C(44)–N(7)	1.346(3)	C(44)–N(7)	1.346(3)
C(45)–C(53)	1.357(4)	C(45)–C(53)	1.357(4)
C(53)–N(7)	1.397(3)	C(53)–N(7)	1.397(3)
2e (95% species)	Bond angle (°)	2e (5% species)	Bond angle (°)
C(44)–Ag(2A)–O(3)	170.37(9)	C(44)–Ag(2B)–O(4)	177.3(3)
		C(44)–Ag(2B)–O(3)	124.5(3)
		O(4)–Ag(2B)–O(3)	55.66(13)
N(7)–C(44)–N(6)	104.5(2)	N(7)–C(44)–N(6)	104.5(2)
N(6)–C(44)–Ag(2A)	131.33(19)	N(6)–C(44)–Ag(2B)	110.5(2)
N(7)–C(44)–Ag(2A)	124.14(18)	N(7)–C(44)–Ag(2B)	141.3(2)
C(44)–N(6)–C(45)	111.3(2)	C(44)–N(6)–C(45)	111.3(2)
C(53)–C(45)–N(6)	106.0(2)	C(53)–C(45)–N(6)	106.0(2)
C(44)–N(7)–C(53)	111.7(2)	C(44)–N(7)–C(53)	111.7(2)
C(45)–C(53)–N(7)	106.6(2)	C(45)–C(53)–N(7)	106.6(2)
C(69)–O(3)–Ag(2A)	107.00(15)	C(69)–O(3)–Ag(2B)	84.9(2)
		C(69)–O(4)–Ag(2B)	94.8(2)
O(4)–C(69)–O(3)	124.5(2)	O(4)–C(69)–O(3)	124.5(2)
O(4)–C(69)–C(70)	120.0(2)	O(4)–C(69)–C(70)	120.0(2)
O(3)–C(69)–C(70)	115.5(2)	O(3)–C(69)–C(70)	115.5(2)

In **2e** one molecule appears as expected [4,17,18,26], and one is split into a major (95%) and a minor (5%) species, therefore suffering from a disorder in the solid state. In the major species the Ag–C bond length is 2.049(2) Å, the Ag–O one is 2.110(2) Å and the C–Ag–O angle is 170.37(9)° as seen in Table 3. This agrees very well with the first molecule, the geometry in **2a** and previously reported examples of this family of compounds reported by our group [17]. The rather short Ag–O distance together with the monodentate

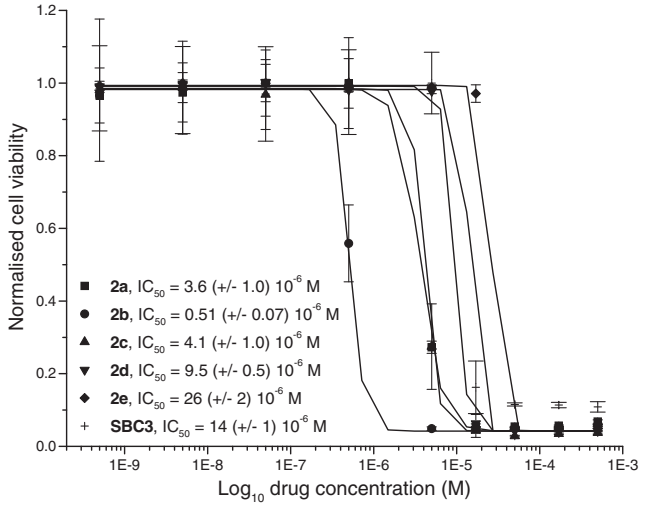

Fig. 4. Cytotoxicity curves from typical MTT assays showing the effect of compounds **2a**–**e** on the viability of Caki-1 cells.

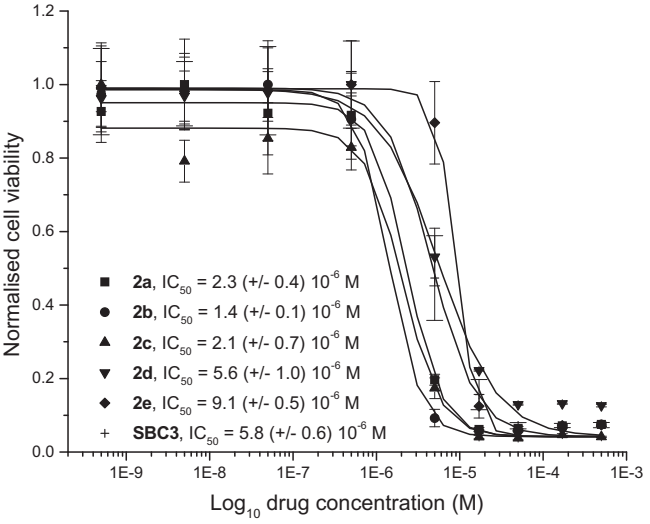

Fig. 5. Cytotoxicity curves from typical MTT assays showing the effect of compounds **2a**–**e** on the viability of MCF-7 cells.

coordination of the acetate to the silver, resulting in a twofold linear coordination of the Ag atom, suggests a predominantly covalent character of the Ag(2A)–O(3) bond.

In the minor species of the second molecule (5%, see Fig. 3) the silver atom binds to both oxygen atoms of the acetate group. The bond length to the carbene carbon atom increases (Ag(2B)–C(44): 2.202(6) Å; Table 3). The bond lengths to the oxygen atoms are elongated as well (Ag(2B)–O(4): 2.274(6) Å, and Ag(2B)–O(3): 2.479(6) Å), increasing the coordination number of silver to 3.This bonding pattern is characteristic for a predominantly ionic coordination of the acetate to the silver. Both of these modes have been observed earlier [17,26] suggesting a rather small energy difference between the major and minor form.

3.3. Biological evaluation

In previous studies, we already synthesized and biologically evaluated symmetrically substituted 1,3-bis-(*p*-substituted-benzyl)-4,5-diarylimidazole silver acetates ([17,21]). From these studies, the earliest reported complex **SBC3** (1,3-bisbenzyl-4,5-bisphenyl-imidazole-2-ylium silver acetate) [21] worked as a lead compound for further substituent optimisation to enhance antibacterial and cytotoxic activity.

3.4. Cytotoxicity studies

The log dose response curves for complexes **2a**–**e** against the human renal cancer cell line Caki-1 and the human breast cancer cell line MCF-7 are shown in Figs. 4 and 5 respectively. All NHC–silver acetate complexes exhibit unique IC_{50} values against both cell lines which indicates that the cytotoxic activity of the compounds is directly influenced by the different *p*-substituents (–H, $–CH_3$, $–OCH_3$, $COOCH_3$, –CN) on the benzyl rings.

The highest activity is observed for compound **2b** with an IC_{50} value of 0.51 (±0.07) μM against Caki-1 and an IC_{50} = 1.4 (±0.1) μM against MCF-7. Compared to our previously reported NHC–silver(I) acetate complexes [17] and especially compared to our lead compound **SBC3** (IC_{50} = 14 (±1) μM against Caki-1 and IC_{50} = 5.8 (±0.6) μM against MCF-7), complex **2b** exhibits a remarkable increase in cytotoxic activity. By removing the CH_3 groups in the *para* position on the benzyl rings, the cytotoxic activity drops by a factor of 6 (**2a**, IC_{50} = 3.0 (±0.6) μM) and replacing it with other groups leads to a decrease in activity of up to 50-fold (**2e**, IC_{50} = 26 (±2) μM). Additionally the IC_{50} value of the NHC precursor **1b**

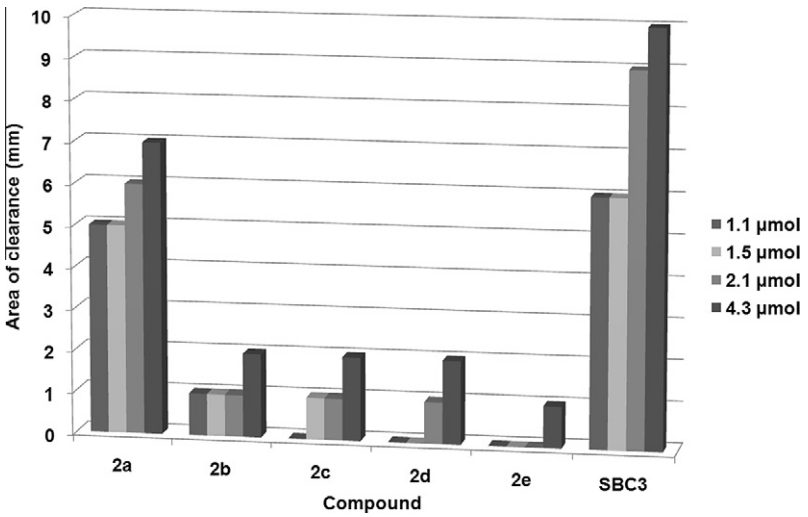

Fig. 6. Area of clearance on *Escherichia coli* (Gram −ve) by **2a**–**e.**

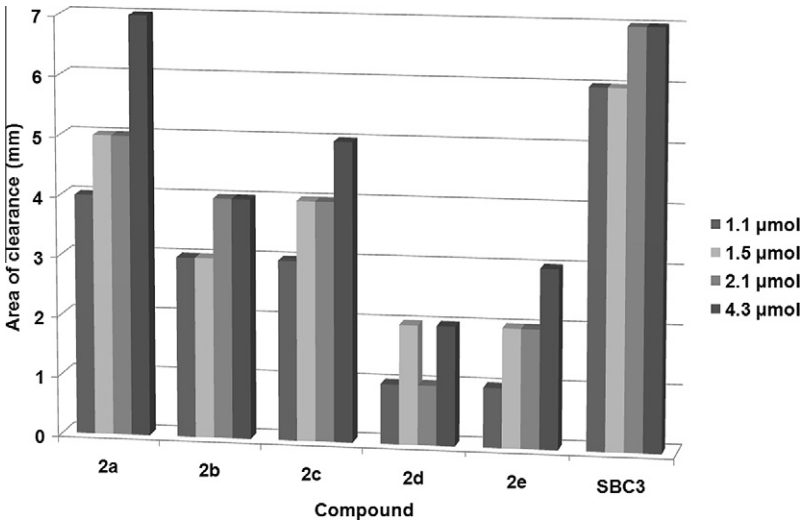

Fig. 7. Area of clearance on *Staphylococcus aureus* (Gram +ve) by **2a–e**.

against Caki-1 was determined to evaluate the effect of silver acetate on the activity of the compound. With an IC_{50} = 4.8 (±0.3) μM **1b** shows a high cytotoxic potential by itself, but in combination with silver acetate, forming the NHC silver(I) complex **2b** the synergistic effect of both parts leads to a superior activity against this particular cell line.

3.5. Antibacterial testing

Using the Kirby–Bauer disk diffusion method, the antibacterial activity of the NHC–silver acetate complexes was tested and summarised in Figs. 6 and 7.

The metal salt (silver(I) acetate) used to prepare the complexes and the solvent (DMSO) used to prepare the stock solutions played no role in growth inhibition on the same bacteria as previously reported [23,26]. An area of clearance of 0 mm was considered as no activity, areas of 1–3 mm as low, 4–7 mm as medium, and areas of clearance $\geqslant$8 mm as high activity.

The primary aim was to synthesise a derivative of **SBC3**, that would exhibit better antimicrobial properties than this leading compound against Gram-positive *S. aureus* (**SBC3**, Area of clearance = 7 mm) and Gram-negative *E. coli* (**SBC3**, Area of clearance = 10 mm) bacteria strains. Almost no antibacterial activity was observed for compounds **2b**, **2d** and **2e** against both bacteria strains. Medium antibacterial activity was observed for compound **2c** against Gram-positive *S. aureus* (Area of clearance = 5 mm) but no antibacterial activity was observed against Gram-negative bacteria *E. coli*. The best antibacterial activity was observed for the compound **2a** against both bacteria strains with an area of clearance of 7 mm (Figs. 6 and 7). Therefore no improvement in antibacterial activity for the herein presented compounds **2a–e** over **SBC3** was observed.

4. Conclusion and outlook

Five new symmetrically substituted *N*-heterocyclic carbene–silver(I) acetate complexes (**2a–e**) were synthesised by the reaction of symmetrically substituted *N*-heterocyclic carbenes (**1a–e**) with silver(I) acetate. Some of the complexes have shown medium to high antibacterial activity, especially against the Gram-positive bacteria strain *S. aureus*, but no improvement in comparison to our lead compound **SBC3** was observed. In contrast to this, the antitumor activity has been greatly enhanced and the NHC–silver complexes **2a–e** yielded IC_{50} values of 3.0 (±0.6), 0.51 (±0.07), 4.2 (±1.2), 9.0 (±0.6), 26 (±2) μM against the Caki-1 renal cancer cell-line (**SBC3** IC_{50} = 14 (±1) μM). At the same time these NHC–silver complexes were found to have IC_{50} values against the human breast cancer cell line MCF-7 of 2.3 (±0.4), 1.4 (±0.2), 3.0 (±0.5), 3.4 (±1.2), 14 (±2) μM, respectively (**SBC3** IC_{50} = 5.8 (±0.6) μM).

One of the compounds presented in this paper, 1,3-bis-(4-methylbenzyl)-4,5-bis-(4-methylphenyl)-imidazole-2-ylidene silver(I) acetate (**2b**) shows the highest cytotoxic activity [IC_{50} = 0.51 (±0.07) μM] compared to all *N*-heterocyclic carbene–silver complexes synthesised by our research group (see [17–22,24–26]). Here the activity of an already cytotoxic imidazolium is strongly enhanced by deprotonation and coordination to silver acetate resulting in a water-soluble and neutral drug molecule. This indicates its high potential as an anticancer drug and gives a good insight into possible further substitution patterns.

Acknowledgement

This project was funded by the UCD School of Chemistry and Chemical Biology.

Appendix A. Supplementary material

CCDC 897777 and 897778 contains the supplementary crystallographic data for **2a** and **2e**. These data can be obtained free of charge from The Cambridge Crystallographic Data Centre via www.ccdc.cam.ac.uk/data_request/cif. Supplementary data associated with this article can be found, in the online version, at http://dx.doi.org/10.1016/j.ica.2012.10.029.

References

[1] I. Ott, R. Gust, Anticancer Agents Med. Chem. 7 (2007) 95.
[2] G. Gasser, I. Ott, N. Metzler-Nolte, J. Med. Chem. 54 (2011) 3.
[3] K.M. Hindi, M.J. Panzner, C.A. Tessier, C.L. Cannon, W.J. Youngs, Chem. Rev. 109 (2009) 3859.
[4] K.M. Hindi, T.J. Siliciano, S. Dumus, M.J. Panzner, D.A. Medvetz, D.V. Reddy, L.A. Hogue, C.E. Hovis, J.K. Hillard, R.J. Mallet, C.A. Tessier, C.L. Cannon, W.J. Youngs, J. Med. Chem. 51 (2008) 1577.
[5] R. Rubbiani, I. Kitanovic, H. Alborzinia, S. Can, A. Kitanovic, L.A. Onambele, M. Stefanopoulou, Y. Geldmacher, W.S. Sheldrick, G. Wolber, A. Prokop, S. Wölfl, I. Ott, J. Med. Chem. 53 (2010) 8608.
[6] M.-L. Teyssot, A.-S. Jarrousse, M. Manin, A. Chevry, S. Roche, F. Norre, C. Beaudoin, L. Morel, D. Boyer, R. Mahiou, A. Gautier, Dalton Trans. (2009) 6894.

[7] M. Skander, P. Retailleau, B. Bourrié, L. Schio, P. Mailliet, A. Marinetti, J. Med. Chem. 53 (2010) 2146.
[8] J.C.Y. Lin, R.T.W. Huang, C.S. Lee, A. Bhattacharyya, W.S. Hwang, I.J.B. Lin, Chem. Rev. 109 (2009) 3561.
[9] J.C. Garrison, W.J. Youngs, Chem. Rev. 105 (2005) 3978.
[10] D.A. Medvetz, K.M. Hindi, M.J. Panzner, A.J. Ditto, Y.H. Yun, W.J. Youngs, Met. Based Drugs (2008) 384010.
[11] A. Melaiye, R.S. Simons, A. Milsted, F. Pingitore, C. Wesdemiotis, C.A. Tessier, W.J. Youngs, J. Med. Chem. 47 (2004) 973.
[12] M.-L. Teyssot, A.-S. Jarrousse, A. Chevry, A. De Haze, C. Beaudoin, M. Manin, S.P. Nolan, S. Díez-González, L. Morel, A. Gautier, Chem. Eur. J. 15 (2009) 314.
[13] A. Kascatan-Nebioglu, A. Melaiye, K.M. Hindi, S. Durmus, M.J. Panzner, L.A. Hogue, R.J. Mallett, C.E. Hovis, M. Coughenour, S.D. Crosby, A. Milsted, D.L. Ely, C.A. Tessier, C.L. Cannon, W.J. Youngs, J. Med. Chem. 49 (2006) 6811.
[14] L. Kaps, B. Biersack, H. Müller-Bunz, K. Mahal, J. Münzner, M. Tacke, T. Mueller, R. Schobert, J. Inorg. Biochem. 106 (2012) 52.
[15] S. Ray, R. Mohan, J.K. Singh, M.K. Samantaray, M.M. Shaikh, D. Panda, P. Ghosh, J. Am. Chem. Soc. 129 (2007) 15042.
[16] W. Liu, K. Bensdorf, A. Hagenbach, U. Abram, B. Niu, A. Mariappan, R. Gust, Eur. J. Med. Chem. 46 (2011) 5927.
[17] F. Hackenberg, G. Lally, H. Müller-Bunz, F. Paradisi, D. Quaglia, W. Streciwilk, M. Tacke, J. Organomet. Chem. 717 (2012) 123.
[18] F. Hackenberg, A. Deally, G. Lally, S. Malenke, H. Müller-Bunz, F. Paradisi, S. Patil, D. Quaglia, M. Tacke, Int. J. Inorg. Chem. (2012) 121540 (13 pp.), http://dx.doi.org/10.1155/2012/121540.
[19] S. Patil, M. Tacke, Coord. Bioinorg. Appl. Inorg. Chem. (2011) 555.
[20] S. Patil, A. Deally, F. Hackenberg, L. Kaps, H. Müller-Bunz, R. Schobert, M. Tacke, Helv. Chim. Acta 94 (2011) 1551.
[21] S. Patil, A. Deally, B. Gleeson, H. Müller-Bunz, F. Paradisi, M. Tacke, Metallomics 3 (2011) 74.
[22] S. Patil, A. Deally, B. Gleeson, F. Hackenberg, H. Müller-Bunz, F. Paradisi, M. Tacke, Z. Anorg. Allg. Chem. 637 (2011) 386.
[23] B. Gleeson, J. Claffey, D. Ertler, M. Hogan, H. Müller-Bunz, F. Paradisi, D. Wallis, M. Tacke, Polyhedron 27 (2008) 3619.
[24] S. Patil, K. Dietrich, A. Deally, B. Gleeson, H. Müller-Bunz, F. Paradisi, M. Tacke, Appl. Organomet. Chem. 24 (2010) 781.
[25] S. Patil, K. Dietrich, A. Deally, B. Gleeson, H. Müller-Bunz, F. Paradisi, M. Tacke, Helv. Chim. Acta 93 (2010) 2347.
[26] S. Patil, J. Claffey, A. Deally, B. Gleeson, M. Hogan, L.M. Menéndez Méndez, H. Müller-Bunz, F. Paradisi, M. Tacke, Eur. J. Inorg. Chem. 2010 (2010) 1020.
[27] CrysalisPro Version 1.171.34.49, Agilent Technologies, 2011.
[28] G.M. Sheldrick, Acta Crystallogr., Sect. A 64 (2008) 112.
[29] H. Bredereck, R. Gompper, D. Hayer, Chem. Ber. 92 (1959) 338.
[30] A. Bondi, H.E. Spaulding, E.D. Smith, C.C. Dietz, Am. J. Med. Sci. 213 (1947) 221.
[31] S.E. Luria, Bacteriol. Rev. 11 (1947) 1.
[32] W.A. Herrmann, C. Köcher, Angew. Chem., Int. Ed. 36 (1997) 2162.
[33] J.C. Garrison, C.A. Tessier, W.J. Youngs, J. Organomet. Chem. 690 (2005) 6008.
[34] M. Viciano, E. Mas-Marzá, M. Sanaú, E. Peris, Organometallics 25 (2006) 3063.
[35] C.P. Newman, G.J. Clarkson, J.P. Rourke, J. Organomet. Chem. 692 (2007) 4962.
[36] V. Lillo, J. Mata, J. Ramírez, E. Peris, E. Fernandez, Organometallics 25 (2006) 5829.
[37] Y. Han, Y.-T. Hong, H.V. Huynh, J. Organomet. Chem. 693 (2008) 3159.
[38] P. de Frémont, N.M. Scott, E.D. Stevens, T. Ramnial, O.C. Lightbody, C.L.B. Macdonald, J.A.C. Clyburne, C.D. Abernethy, S.P. Nolan, Organometallics 24 (2005) 6301.